



In situ N₂-NH₃ plasma pre-treatment of silicon substrate enhances the initial growth and restricts the substrate oxidation during alumina ALD

Georgios Gakis, Hugues Vergnes, Fuccio Cristiano, Yann Tison, Constantin Vahlas, Brigitte Caussat, Andreas Boudouvis, Emmanuel Scheid

► To cite this version:

Georgios Gakis, Hugues Vergnes, Fuccio Cristiano, Yann Tison, Constantin Vahlas, et al.. In situ N₂-NH₃ plasma pre-treatment of silicon substrate enhances the initial growth and restricts the substrate oxidation during alumina ALD. Journal of Applied Physics, 2019, 126 (12), pp.125305. 10.1063/1.5113755 . hal-02396236

HAL Id: hal-02396236

<https://hal.science/hal-02396236>

Submitted on 5 Dec 2019


HAL is a multi-disciplinary open access archive for the deposit and dissemination of scientific research documents, whether they are published or not. The documents may come from teaching and research institutions in France or abroad, or from public or private research centers.

L'archive ouverte pluridisciplinaire **HAL**, est destinée au dépôt et à la diffusion de documents scientifiques de niveau recherche, publiés ou non, émanant des établissements d'enseignement et de recherche français ou étrangers, des laboratoires publics ou privés.

#n situ N₂-NH₃ plasma pre-treatment of silicon substrate enhances the initial growth and restricts the substrate oxidation during alumina ALD

Cite as: J. Appl. Phys. **126**, 125305 (2019); <https://doi.org/10.1063/1.5113755>

Submitted: 07 June 2019 . Accepted: 06 September 2019 . Published Online: 26 September 2019

Georgios P. Gakis, Hugues Vergnes , Fuccio Cristiano, Yann Tison , Constantin Vahlas , Brigitte Caussat , Andreas G. Boudouvis, and Emmanuel Scheid 



View Online



Export Citation



CrossMark

ARTICLES YOU MAY BE INTERESTED IN

[Role of device architecture and AlO_x interlayer in organic Schottky diodes and their interpretation by analytical modeling](#)

Journal of Applied Physics **126**, 125501 (2019); <https://doi.org/10.1063/1.5109083>

[Modeling ballistic phonon transport from a cylindrical electron beam heat source](#)

Journal of Applied Physics **126**, 124306 (2019); <https://doi.org/10.1063/1.5115165>

[Nonreciprocity and thermoelectric performance in a double-dot Aharonov–Bohm interferometer](#)

Journal of Applied Physics **126**, 124305 (2019); <https://doi.org/10.1063/1.5111181>

Lock-in Amplifiers up to 600 MHz

starting at
\$6,210



 Zurich
Instruments

Watch the Video 

In situ N₂-NH₃ plasma pre-treatment of silicon substrate enhances the initial growth and restricts the substrate oxidation during alumina ALD

Cite as: J. Appl. Phys. 126, 125305 (2019); doi: 10.1063/1.5113755

Submitted: 7 June 2019 · Accepted: 6 September 2019 ·

Published Online: 26 September 2019



Georgios P. Gakis,^{1,2} Hugues Vergnes,² Fuccio Cristiano,³ Yann Tison,⁴ Constantin Vahlas,⁵ Brigitte Caussat,² Andreas G. Boudouvis,¹ and Emmanuel Scheid^{3,a)}

AFFILIATIONS

¹School of Chemical Engineering, National Technical University of Athens, Heroon Polytechniou 9, 15780 Zografou, Athens, Greece

²Laboratoire de Génie Chimique, Université de Toulouse, 4 allée Emile Monso, 31030 Toulouse cedex 4, France

³LAAS, Université de Toulouse, 7 avenue du Colonel Roche, 31031 Toulouse, France

⁴IPREM, Université de Pau et des Pays de l'Adour, Hélioparc Pau-Pyrénées, 2 Avenue du Président Angot, 64053 Pau Cedex 9, France

⁵CIRIMAT, Université de Toulouse, 4 allée Emile Monso, 31030 Toulouse cedex 4, France

^{a)}Author to whom correspondence should be addressed: scheid@laas.fr. Tel.: +33 561336485.

ABSTRACT

The initial substrate inhibiting island growth and the formation of an interfacial layer with uncontrollable characteristics are the two main drawbacks of the Atomic Layer Deposition (ALD) of high-k metal-oxide gate dielectrics on silicon (Si). In this paper, we investigate the ALD of Al₂O₃ films from trimethyl aluminum and H₂O, on fluorhydric acid (HF) cleaned, as well as on HF-cleaned and *in situ* N₂-NH₃ plasma pretreated Si between 0 and 75 cycles. The films and their interface were characterized via Scanning Transmission Electron Microscopy coupled to Energy-Dispersive X-ray spectroscopy. The initial deposition is clearly increased on the pretreated surfaces, obtaining a linear ALD regime even after 5 ALD cycles, compared to several tens of cycles needed on HF-cleaned Si. Furthermore, a Si_xN_y layer is formed by the N₂-NH₃ plasma pretreatment, which acts as a barrier layer, reducing the oxidation of the Si substrate beneath it. This analysis provides a general framework for the understanding and determination of adequate surface pretreatments, able to combat the substrate inhibited initial growth and the Si oxidation during metal-oxide ALD on Si.

Published under license by AIP Publishing. <https://doi.org/10.1063/1.5113755>

INTRODUCTION

The growing integration of the electronic devices has led to the constant shrinking of the feature size of metal-oxide-semiconductor field effect transistors (MOSFETs). This has reinforced the need for the production of conformal ultrathin film structures.¹ The high-k gate oxides used for the transistor gate stack in microelectronic devices need to be highly uniform and pinhole-free on the semiconductors (Si) to prevent leakage current.¹ In this context, the Atomic Layer Deposition (ALD) process² has emerged as the appropriate tool to produce such films. A high control over the deposited film thickness, uniformity, and composition purity can be obtained due to the self-limiting nature of the involved reactions.^{2,3}

Al₂O₃ is a favorable candidate to replace SiO₂ as a high-k layer. Its higher dielectric constant (Al₂O₃: $k = 9$, SiO₂: $k = 3.8$ ⁴)

and similar bandgap⁴ make it an appropriate dielectric material for microelectronic applications. The deposition of Al₂O₃ films, using trimethyl aluminum [Al(CH₃)₃, TMA] and H₂O vapor as a metal precursor and an oxidant source, respectively,⁵ is one of the most studied ALD processes. Works published on this ALD process revealed important aspects of the deposition process,^{5–7} reaction mechanisms,^{8–11} reaction kinetics^{12,13} as well as the ALD reactor dynamics.^{13–15}

However, despite the numerous studies available, uncontrolled phenomena still occur in this process. First, the H-terminated Si species resulting from the standard *ex situ* HF pretreatment of the Si substrate are initially nonreactive toward both of the reactants.^{10,16} Hence, the deposition during the first tens of ALD cycles is inhibited by the substrate reactivity and initially takes place on

surface defects.^{16,19} During subsequent cycles, the film preferentially deposits on the already deposited material. As a consequence, the initial deposition of Al_2O_3 takes place in the island, instead of layer-by-layer, growth mode, prior to coalescence, and formation of the continuous film.^{18–20} From this point onwards, the deposition can indeed proceed in the ALD linear growth regime, with a constant film growth per cycle (GPC).^{3,18,19} Consequently, for the deposition of a continuous film, this nucleation process requires a minimum of around 20 ALD cycles.¹⁸

Another aspect is the formation of an interfacial layer between the ALD film and the Si substrate. This interface has a negative impact, as it affects the electrical properties of the deposited structure, exhibiting a low dielectric constant and high leakage current for thin films below 4 nm,²¹ thus limiting the interest for potential applications of such films. Works have been published that investigate the composition and thickness of this layer,^{4,22,23} which appears to consist of Si oxides in various oxidation states,^{4,20,22} Al-silicates,⁴ and OH species.^{20,22,23}

It is clear that to achieve the production of sharp, pure nanometric-thick films, the two main drawbacks due to the nucleation delay and island growth as well as the reactive diffusion between the substrate and the film must be reduced. The deposition needs to rapidly attain the layer-by-layer ALD regime, with no island regime prevailing period during the first cycles, while the Si interfacial oxidation must be restricted as much as possible. For this, different research groups have investigated various Si surface pretreatments and their effects on the initial deposition steps and substrate reactivity. Frank *et al.*¹⁶ used a 10^8 Langmuir TMA exposure prior to TMA + H_2O ALD and reported an increased initial film growth. According to Xu *et al.*,²⁴ this pretreatment can also reduce the interfacial SiO_x formation. Damlencourt *et al.*²⁵ used a Cl_2 + H_2O treatment after the HF pretreatment of the Si surface to create a surface monolayer of OH groups and observed an increased film growth during the first ALD cycles.

Brewer *et al.*²⁶ used a thermal treatment based on a N_2 - NH_3 gas mixture, leading to the formation of a Si_xN_y layer. They obtained an increased growth during the first steps of Al_2O_3 deposition and a limited SiO_x formation. Xu *et al.*²⁷ compared samples pretreated with N_2 - NH_3 plasma with those pretreated using a long TMA exposure. In both cases, the substrate oxidation was restricted, and the deposition was increased, a result also shown by Lu *et al.*,²⁸ who used the same pretreatment. They also showed that the N_2 - NH_3 plasma pretreatment leads to interfaces with better thermal stability, lower leakage current, and smaller capacitance-voltage (CV) hysteresis.²⁷

From the above works,^{26,27} it is clear that the N_2 - NH_3 pretreatment of the Si surface would be a promising option to combat these drawbacks of Al_2O_3 ALD. However, more insight is required concerning the use of this pretreatment. Brewer *et al.*²⁶ have studied the deposition increase deduced from IR absorbance spectra, for only the first five ALD cycles. It is worth noting that in their work, the ALD deposition temperature was between 318 and 380 °C, which is above the maximum temperature of the ALD window for the TMA + H_2O process (300 °C).³ Xu *et al.*²⁷ have performed their study only for 35 cycles. An analysis of the evolution of the film deposition and interfacial SiO_x formation during a large number of ALD cycles remains to be performed.

Furthermore, there is a need to investigate the involved mechanisms in more detail.

In this work, we deposit Al_2O_3 films from TMA and H_2O on HF-cleaned and *in situ* N_2 - NH_3 plasma pretreated Si wafers, in a commercial ALD reactor. We previously reported on the reactor behavior, process dynamics as well as the reaction kinetics during the ALD ideal regime.^{13,14} We characterize the films by STEM to study both the Al_2O_3 deposition rate and the Si oxidation evolution between 0 and 75 cycles. We use theoretical results from the literature to explain the enhanced deposition rate and the surface mechanisms in the case of the N_2 - NH_3 pretreated Si. The deposition reaction kinetics are discussed through the calculation of reaction probabilities, based on activation energies previously presented in the existing literature. We analyze the local chemical composition by performing STEM-energy-dispersive X-ray (EDX) characterizations along the depth of the film. We investigate the substrate oxidation, by performing XPS characterizations. Finally, we discuss the reduced interfacial SiO_x formation and the nature of the interface.

EXPERIMENTAL METHODS

The Al_2O_3 films were deposited on 100 mm diameter Si (100) wafers in a commercial Veeco® Fiji F200 ALD setup. The Si (100) wafers were pretreated by de-ionized (DI) water rinsing, followed by dipping in a 5% HF solution for 1 min, to obtain native oxide removal from the Si surface, and a final DI water rinsing. After the cleaning procedure, the wafer was dried and immediately loaded into the chamber, which was pumped out to vacuum pressure (10^{-4} – 10^{-5} Torr) during 10 min. Two sets of samples were studied. The first set of samples, hereafter called nonpretreated samples (NPT), is Si (100) wafers on which ALD is directly performed after the HF cleaning procedure described above. The second set of samples, hereafter called N_2 - NH_3 plasma pretreated samples (PT), is Si (100) wafers on which after the HF cleaning, an *in situ* N_2 - NH_3 plasma pretreatment is performed prior to ALD.

For the NPT samples, the base pressure was then set to that of the ALD process (0.072 Torr) during 5 min, before starting the deposition. For the PT set of samples, the Si (100) wafers were exposed to 120 sccm of an N_2 - NH_3 (electronic grade gases, Air Liquide) gas mixture (16.67% NH_3), without plasma, at 0.08 Torr, during 5 min. Then, the plasma was activated for 1 min. The samples were heated at 300 °C during the pretreatment. Through the precursor line, 10 sccm of Ar (electronic grade gas, Air Liquide) were also fed during the pretreatment, in order to avoid retrodiffusion toward the ALD valves. After the pretreatment, the N_2 - NH_3 plasma mixture feed was stopped, and the nominal Ar flows and the base pressure of the ALD process (0.072 Torr) were set during a transition time of 5 min, prior to starting the ALD process.

For the ALD of Al_2O_3 , TMA (purity: >97%, Sigma Aldrich) and DI H_2O were used as reactants. Ar (180 sccm) was used as both carrier and purging gases, entering the reactor through three inlets. More information on the reactor geometry and process setup is available in our previous works.^{13,14} The TMA pulse time was set to 0.025 s, while the water pulse was 0.1 s. The two reactant exposures were separated by an Ar purging step of 5 s. With the pulsing and purging times being set, the isolation valve of the capacitance manometer was closed, and the process was initiated. The number

of cycles used varied from 5 to 75. The substrate temperature was kept at 300 °C and the base pressure at 0.072 Torr, in all experiments. This process recipe has been previously used and leads to an ALD growth with a GPC of ~ 0.1 nm/cycle,¹³ once the process has attained the linear growth regime.

The samples were characterized by Transmission Electron Microscopy (TEM) using a 200 kV JEOL Cold FEG probe-corrected ARM200F microscope for either High Resolution (HREM) or Scanning TEM (STEM) analysis. STEM images were recorded in both Bright-Field (BF) and High Angle Annular Dark-Field (HAADF) conditions. Chemical characterization was performed by Energy-dispersive X-ray (EDX) spectroscopy in the STEM mode. The TEM cross-sectional lamellas were prepared by Focused Ion Beam (FIB) in a FEI Helios Nanolab 600i dual beam SEM/FIB. For the STEM analysis, all the samples were capped with a 200 nm carbon layer using an electron beam, followed by a 3 μ m PT layer deposited with an ion beam.

X-ray photoelectron spectroscopy (XPS) was performed in a Thermo K α XPS system in order to study the chemical nature of the film bulk and interface. XPS was performed using an Al K α source (1486.7 eV) with a 20 eV pass energy, while the XPS binding energy scale was calibrated by the adventitious C 1s peak at 285.0 eV. Curve fitting has been performed using CasaXPS[®]; for 1s core peaks (O 1s, C 1s), a single peak has been used for each chemical environment, while doublets have been used for 2p core peaks, accounting for spin-orbit coupling.

RESULTS

Si surface pretreatment

Figure 1(a) presents a STEM-HAADF image taken from the N₂-NH₃ plasma pretreated Si (100) samples, with no Al₂O₃ deposition. It appears that an amorphous layer has been formed due to the pretreatment on the Si surface [the PT layer in Fig. 1(a)], whose thickness is ~ 1.8 nm.

Brewer *et al.*²⁶ reported the formation of a Si_xN_y layer after the exposure of Si to N₂-NH₃, at temperatures above 380 °C. In the present case, even at 300 °C, it is evident that an amorphous layer

is formed on the Si surface. This is due to the use of N₂-NH₃ plasma, instead of thermal nitridation with N₂-NH₃. Furthermore, in the work of Brewer *et al.*,²⁶ the plasma N₂-NH₃ gas mixture for the pretreatment had a lower NH₃ molar composition (4%) compared to the present study (16.67%).

To investigate the layer composition, EDX analysis along the layer depth was performed. The EDX profiles (raw count data) for N, Si, and O species along the length of the layer are shown in Fig. 1(b). It appears that a layer consisting of Si and N is present after the N₂-NH₃ plasma pretreatment on the Si substrate surface. The layer also consists of a significant amount of O, along its whole thickness. A sharp increase of the O signal is detected at the interface between the Si substrate and the PT layer. This O content could come from subsequent oxidation of the layer, due to its exposure to air after the sample was taken out from the chamber. It could also be assigned to native SiO_x, which was not removed during the HF cleaning. However, EDX analysis performed on an HF-cleaned Si substrate, under the same conditions, showed in our previous work,²⁰ showed no oxidation of the Si substrate, revealing the good passivation of the Si substrate by the HF pretreatment. This shows that the PT layer formed by the *in situ* N₂-NH₃ pretreatment is probably oxidized after its exposure to atmospheric O.

Although Si_xN_y is known to be an oxygen diffusion barrier,²⁹ in the present case, the layer is nonetheless oxidized. This behavior is attributed to the poor stoichiometry and low density of the layer. The layer could also contain amounts of H (not detectable by EDX) coming from NH₃ decomposition within the plasma. These features make the layer porous, which facilitates O diffusion. Such oxidation of the PT layer was also reported by Brewer *et al.*²⁶ However, by analyzing several EDX profiles similar to the one shown in Fig. 1(b), it is found that, when moving from the Si substrate toward the C capping layer, the increase in the O and N profiles is such that their half-maximum position occurs at the same depth. This suggests that although the PT layer is oxidized, the oxidation of the substrate itself and the formation of an interfacial SiO_x layer can be neglected, i.e., the Si surface is protected from oxidation by the formed layer.

Further characterization of this layer composition was made by XPS (Fig. 2). The XPS spectrum exhibits a O 1s peak at 532.8 eV, attributed to oxygen in a SiO_x environment; a N 1s peak at 398.0 eV, attributed to nitrogen in a Si₃N₄ environment;³⁶ and a Si 2p doublet peak [blue continuous and dashed lines in Fig. 2(b)] at ~ 99.2 eV, corresponding to Si⁰.

A second peak is revealed by the Si 2p spectra, situated at a higher binding energy of ~ 103.3 eV. The peak deconvolution was done using two double peaks, one at ~ 103.2 eV (orange continuous and dashed lines) and one at ~ 101.9 eV (green continuous and dashed lines). The first peak corresponds to an energy shift of ~ 4.1 eV from Si⁰ and is assigned to oxidized Si in higher oxidation states,^{4,20} such as Si³⁺ and Si⁴⁺. The second peak (energy shift of ~ 2.7 eV) can be assigned to Si-N bonds,³⁶ with some contributions from Si in lower oxidation states, such as SiO_x species or Si-O-N bonds.^{4,20} It is to be noted that neither Si-H nor clear N-H peak are observed. A detailed discussion of the N 1s, C 1s, and O 1s XPS core level peak and the surface composition obtained for this pretreated sample can be found in Fig. S1 and Table S1 of the [supplementary material](#).

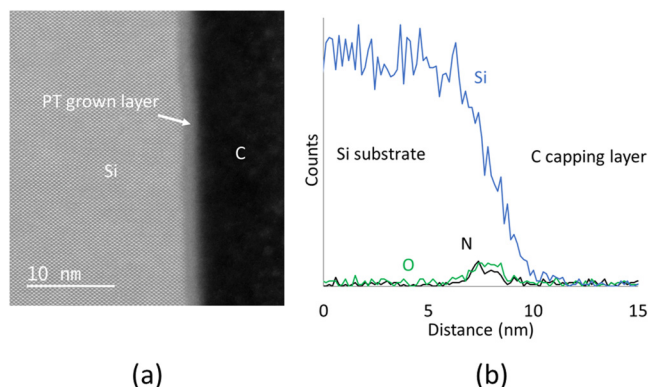


FIG. 1. (a) STEM image of the NH₃ plasma pretreated substrate and (b) EDX analysis along the film depth: N (black), O (green), and Si (blue) depth profiles.

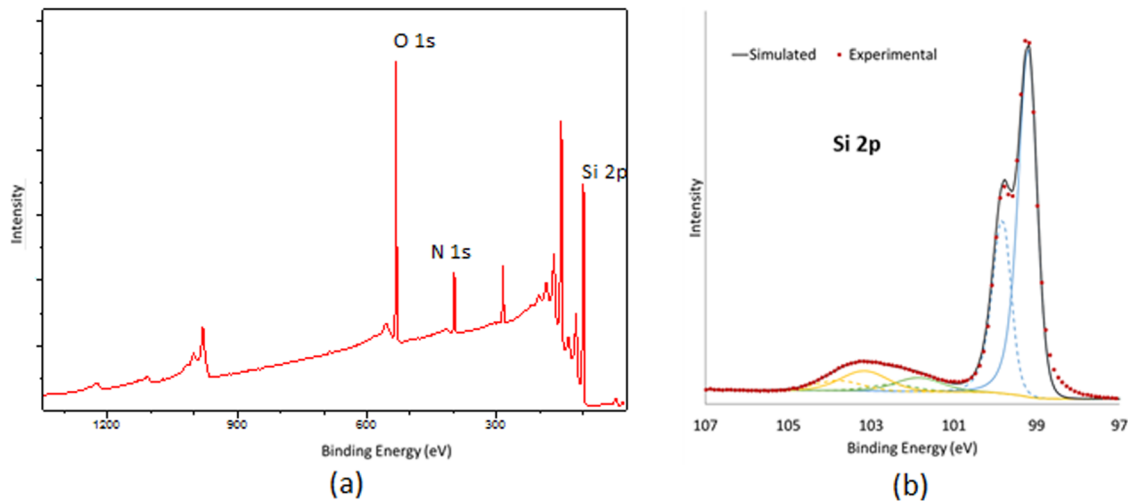


FIG. 2. (a) XPS experimental spectrum of the pretreated Si substrate and (b) Zoom on Si 2p peak: Experimental and simulated.

In order to investigate the source of the layer oxidation, an *in situ* ALD capping by an AlN layer of a plasma N_2 - NH_3 pretreated Si substrate was performed. As this *in situ* process does not involve any oxygen, it is adequate to reveal the source of the PT layer oxidation shown in Fig. 1. The resulting STEM-HAADF image and EDX analysis are shown in Fig. 3.

A PT layer is still observed between the Si substrate and the AlN capping layer, as indicated by the thin dark contrast layer located at the Si surface in Fig. 3(a), whose thickness is ~ 1.1 nm. The elemental EDX profiles in Fig. 3(b) show that O atoms are

contained in the AlN layer, with a maximum oxygen concentration located at the surface. Since the deposition does not involve any oxygen source, we conclude that oxidation of the AlN layer occurs during the subsequent exposure to ambient air. In addition, the O content is low in the PT layer, as the O counts near the interface with Si are very low. No sharp increase of the O signal is detected at the interface between the Si substrate and the PT layer. These results suggest that no oxidation of the PT layer occurs in the presence of a capping layer and that the amount of O detected in the AlN layer is due to diffused O from the AlN layer surface. We can

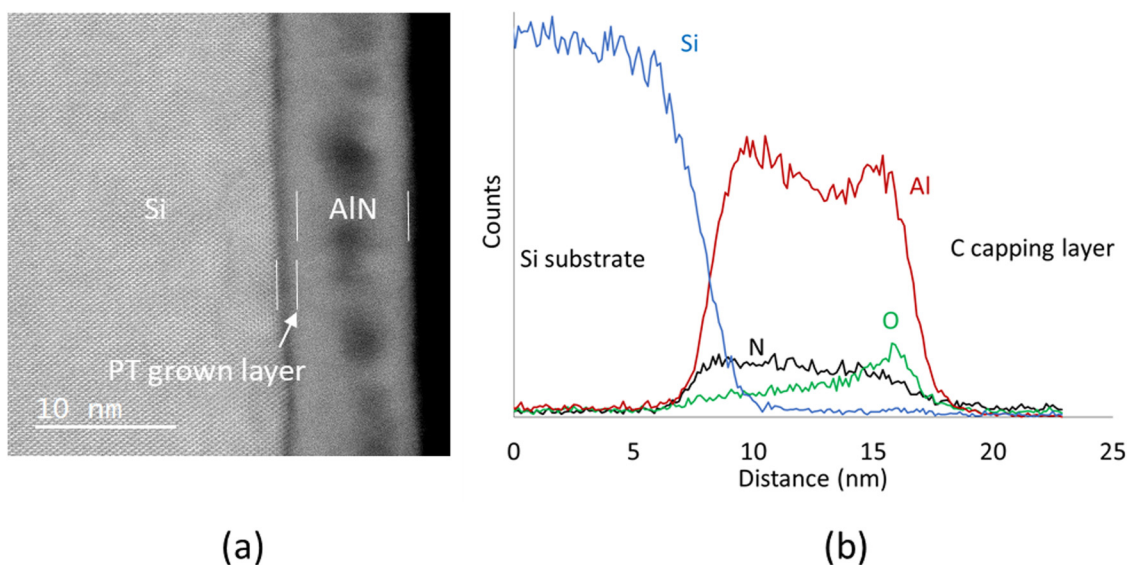


FIG. 3. (a) STEM image and (b) EDX analysis along the film depth of the pretreated Si substrate after AlN capping.

then conclude that the oxidation of the PT layer previously observed in the uncapped sample [Fig. 1(b)] is mainly due to the exposure to ambient air (after deposition). Hence, we assume that a Si_xN_y layer has been formed by the pretreatment.

The oxidized Si_xN_y layer thickness measured in Fig. 1 was of ~ 1.8 nm, which means that a slight increase in the thickness could occur due to oxidation. However, this is expected to be the case during ALD, as H_2O can also oxidize the layer.²⁶ Hence, for subsequent discussion, the PT layer thickness formed by the pretreatment will be considered to be ~ 1.8 nm.

Morphological and chemical characterizations of ALD Al_2O_3 films

To study the effect of the N_2 - NH_3 plasma pretreatment on the ALD growth, the Al_2O_3 films deposited using 5, 20, and 75 ALD cycles, on NPT and PT Si, were analyzed by STEM-HAADF, as

presented in Fig. 4. The Al_2O_3 thickness on the NPT and the PT Si was measured by STEM and is also plotted in Fig. 4 (top diagram). For the Al_2O_3 films deposited on the PT Si, the thickness is deduced by subtracting that of the PT layer (~ 1.8 nm, Fig. 1). In our previous work,²⁰ we measured the thicknesses of the ALD films and their interface by X-ray reflectivity (XRR) STEM and TEM. The good agreement between the STEM-HAADF and the other techniques shows that the STEM-HAADF analysis is reliable for the thickness measurement of the samples. The derived GPC is also presented in Fig. 3 (bottom diagram). Since the number of the NPT samples is limited, the error for the GPC estimation is rather high. Hence, the GPC derived from XRR measurements,²⁰ for the same process conditions, is also presented in Fig. 4.

In order to study the efficiency of the N_2 - NH_3 plasma pretreatment on the Si substrate oxidation, the respective profiles of the EDX counts of Si, O, Al, and N species along the film depth for films deposited on both NPT and PT Si surfaces are presented in Fig. 5.

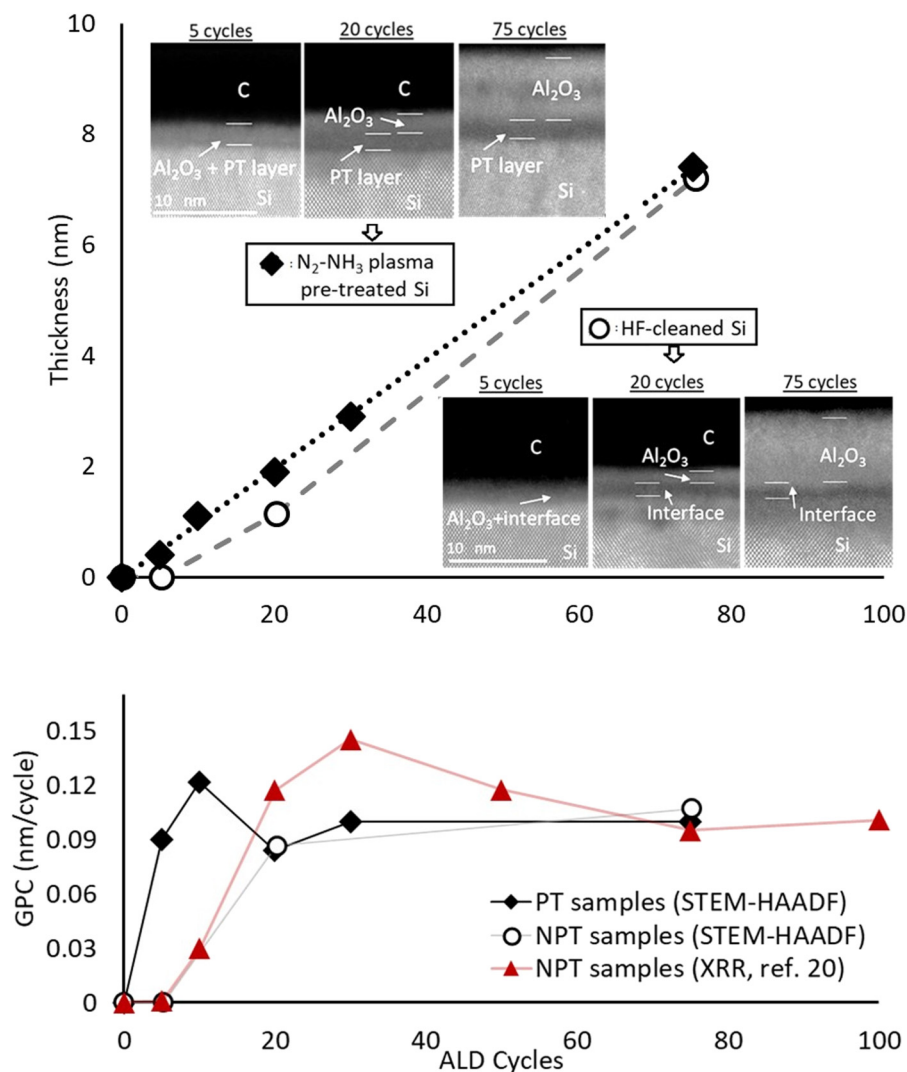


FIG. 4. Top diagram: Dark-field STEM images of the ALD samples and the derived thickness as a function of ALD cycles on NPT and N_2 - NH_3 plasma PT Si surfaces. Bottom diagram: GPC derived from the thickness measurements.

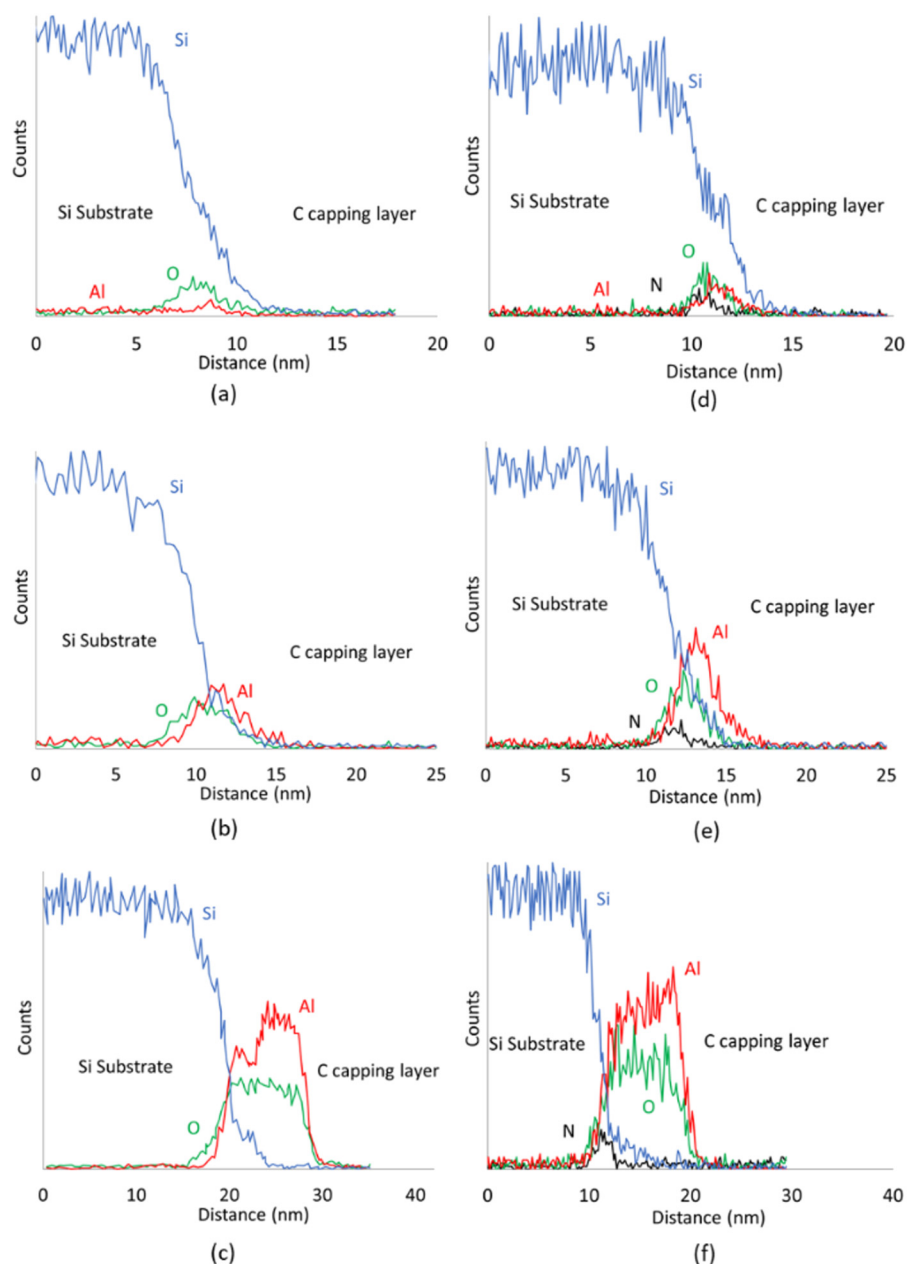


FIG. 5. EDX count profiles for Al, Si, O, and N species of the ALD films: Left column: NPT Si surfaces: (a) 5 cycles, (b) 20 cycles, and (c) 75 cycles. Right column: $\text{N}_2\text{-NH}_3$ plasma PT Si surfaces: (d) 5 cycles, (e) 20 cycles, and (f) 75 cycles.

Figure 4 shows that after 5 ALD cycles, no clear continuous deposition of Al_2O_3 is observable on the NPT samples. This confirms the low reactivity of the H-terminated surface resulting from the HF cleaning toward the ALD reactants. In order to deposit a continuous layer, more ALD cycles are needed. Indeed, EDX characterizations [Fig. 5(a)] show that after 5 ALD cycles on the NPT Si surface, only a very small amount of Al can be traced on the Si surface. This confirms that the Si surface is highly passivated toward TMA by the HF cleaning, which leaves the surface H-terminated. This low reactivity has previously been discussed in

the literature;^{10,16,17} it results in island growth during the first ALD cycles^{18–20} and explains the low detection of Al in Fig. 5(a), as after 5 cycles, the film is not continuous yet. We confirmed this behavior by XRR measurements combined with an island growth model.²⁰ The low reactivity of the initial Si surface is further discussed in the Discussion section.

Si oxidation, however, occurred as seen by the clear rise of the O counts when moving from the Si substrate toward the C capping layer [Fig. 5(a)]. This oxidation can be due to the sample exposure to the atmosphere after the deposition or to oxidation from H_2O .

The presence of Al on the surface is known to catalyze the Si oxidation.^{17,31} Hence, a small amount of Al deposited on the surface could lead to the oxidation of nearby Si. The thickness of the oxidized Si layer is ~ 1.9 nm. The mechanism for the Si oxidation involves the formation of Al-OH and Si-OH species during the island growth regime, catalyzed by the presence of Al on the surface. This has been shown and discussed for the NPT samples, using XPS and SIMS measurements.²⁰

After 20 cycles on NPT, a deposited layer with a brighter contrast attributed to Al_2O_3 can be seen on the STEM micrograph. This layer has a thickness of ~ 1.3 nm, measured from the STEM image. The fact that the layer has a surface roughness and a varying contrast along its length could mean that it is not continuous yet. This is consistent with the results of Puurunen *et al.*,¹⁸ who reported that after 20 cycles, the deposited film is not yet continuous, due to the island growth regime during the first cycles of deposition. Furthermore, an interfacial layer of ~ 1.6 nm appears between the deposited Al_2O_3 and the Si substrate. This layer, consisting mainly of Si oxides [Fig. 5(b)], is formed by Si oxidation from H_2O during the ALD island formation as well as through interdiffusion between Si and the ALD deposited layer.²² This interfacial layer has been analyzed by XPS, EDX, and SIMS for the NPT samples²⁰ and showed that it consists of Si oxides in various oxidation states as well as Al-silicates.

After 75 cycles on NPT, a ~ 7.2 nm layer of Al_2O_3 is deposited (Fig. 4). An increase of the Si substrate oxidation is also observed, as the interfacial oxide layer has grown to ~ 2.4 nm. The Si surface on the 75 cycle sample is also rougher than on the other two samples. This could lead to a higher apparent thickness of the interfacial oxide. Nevertheless, the increase in the interface thickness is clear between 20 and 75 cycles.

In both the 20 and 75 cycle samples on NPT, moving from the Si substrate to the C capping layer, the O counts rise before the respective Al counts [Figs. 5(b) and 5(c), respectively]. This shows that there is an interface between the deposited film and the Si substrate, which consists of oxidized Si. For the 20 cycle sample on NPT, this layer consists of ~ 1.5 nm of SiO_x and ~ 0.7 nm of a region where Si, O, and Al species are simultaneously present, as estimated from the full width at half maximum (FWHM) of the element counts. For the sample deposited using 75 cycles on NPT, the Si oxidized layer consists of ~ 1 nm SiO_x and ~ 1.4 nm of the Si, O, and Al region. These values are consistent with the STEM measurements (Fig. 4) and are close to values reported by previous works.^{27,30} These results show the formation of a $\text{Si}_x\text{O}_y\text{Al}$ layer, probably created through interdiffusion of species during ALD. The presence of $\text{Si}_x\text{O}_y\text{Al}$ was also shown by XPS and SIMS analysis of the NPT samples.²⁰

When the $\text{N}_2\text{-NH}_3$ plasma pretreatment is performed prior to deposition, the STEM images show that even after 5 ALD cycles (Fig. 4), a ~ 2.2 nm thick layer has been deposited. A clear Al count peak can be seen on the respective EDX counts [Fig. 5(d)], moving from the Si substrate to the C capping layer. We can deduce from the deposition of Al that the $\text{N}_2\text{-NH}_3$ plasma pretreatment is efficient in enhancing the reactivity of the surface, thanks to the formation of the PT Si_xN_y layer. The contrast difference between the PT layer and the ALD Al_2O_3 film is not clear. The Al_2O_3 thickness can be obtained by subtracting the ~ 1.8 nm layer measured

for the sample without deposition [Fig. 1(a)], from the total layer thickness. This leads to a value of ~ 0.4 nm.

Figure 5(d) also shows a significant reduction of the Si oxidation. No region is detected, where only Si and O species are present. A layer of Si, O, and N appears, with a thickness of ~ 1 nm, using the FWHM. The presence of Al cannot be excluded within this region; however, the EDX Al counts are low. Then, a region of ~ 0.8 nm is measured where Si, O, Al, and N are all present. Al diffusion and deposition in the less dense Si_xN_y layer could explain this result, as the fact that although the less dense amorphous PT layer could not be easily observable by STEM [Fig. 1(a)], the layer with 5 ALD cycles could be distinct with a darker contrast (Fig. 3).

After 20 and 75 cycles on the PT Si surfaces (Fig. 4), the total deposited film thickness reaches ~ 3.7 nm and ~ 9.1 nm, respectively, which correspond to a thickness increase of ~ 1.9 nm and ~ 7.3 nm, respectively, compared to the PT layer. As the brighter contrast Al_2O_3 film is deposited, the contrast difference between the PT layer and Al_2O_3 becomes clearer and the two layers can be identified. The Si substrate oxidation [Figs. 5(e) and 5(f)] is reduced compared to the respective NPT samples [Figs. 5(b) and 5(c)]. For the 20 cycle sample, the SiONH region thickness is ~ 1 nm, using the FWHM. Between the Si-O-N-H layer and the deposited Al_2O_3 film, a region of Si, N, Al, and O exists with a thickness of 0.8 nm. The respective SiONH for the 75 cycle sample is ~ 0.5 nm thick, while the region of Si, N, Al, and O has a thickness of ~ 1 nm.

The above results show an enhanced deposition on the PT Si surfaces during the first ALD cycles, in comparison with the NPT Si surfaces. For the NPT substrates, no unambiguous film deposition is observable after 5 cycles, while the averaged GPC is only of ~ 0.07 nm/cycle after 20 cycles and reaches ~ 0.1 nm/cycle between 20 and 75 cycles. On the PT substrates, the mean GPC is ~ 0.1 nm/cycle between 5 and 75 cycles, which is the GPC obtained at 300°C during the steady ALD regime in our process setup.¹³ This mean value was also found by STEM measurements on samples deposited after 10 and 30 cycles (not shown) on the PT samples. Hence, the island growth regime period, reported to occur during the first ALD cycles,^{3,16–20} has successfully been restricted by using the $\text{N}_2\text{-NH}_3$ plasma pretreatment of the Si surface.

Furthermore, the results of Fig. 5 show a significant reduction of the substrate oxidation, in comparison with the NPT samples. This reduction is attributed to the barrier properties of the Si_xN_y layer against oxygen diffusion. Figure 1(b) shows that although the Si_xN_y layer is oxidized, the Si surface beneath the PT layer is protected, and the SiO_x layer formation is reduced.

In order to confirm this low substrate oxidation on PT samples, XPS characterizations were also performed on a PT Si sample with 20 ALD cycles of TMA/ H_2O . The Si 2p XPS spectra and their deconvolution are shown in Fig. 6.

It shows that the Si 2p XPS spectra exhibit a doublet peak (blue continuous and dashed lines) at ~ 99.1 eV, corresponding to Si^0 . It can be seen (Fig. 6) that the second peak in the Si 2p spectra is now situated at 101.7 eV. For this peak deconvolution, only a doublet peak at 101.6 eV was used (green continuous and dashed lines, energy shift of ~ 2.5 eV).

Si in higher oxidation states was hence not detected on the 20 cycle PT sample, while the peak is assigned mainly to Si-N

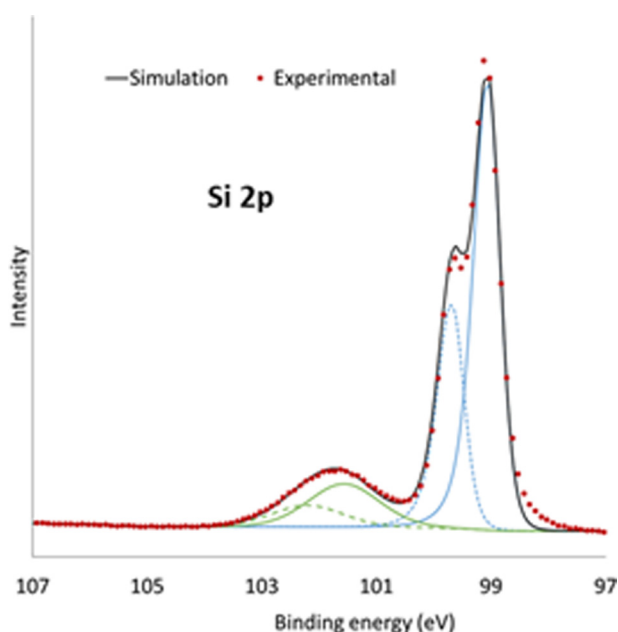


FIG. 6. Si 2p XPS spectra for PT Si sample with 20 cycle ALD. Experimental and simulated.

bonds,³⁶ with some contributions from Si in lower oxidation states, such as SiO_x species, Si–O–Al, or Si–O–N bonds. It is evident from Fig. 5 that the Si oxidation was reduced when 20 cycles of ALD were performed. This shows the barrier properties of the Al_2O_3 film in reducing the substrate oxidation.

XPS characterizations of ALD deposited Al_2O_3 films on NPT Si revealed main peaks situated ~ 3.4 eV higher in energy than the Si^0 main peak, with the main contribution being from higher Si oxidation states.²⁰ In Fig. 6, it is seen that this energy shift is lower (~ 2.5 eV), and the main contribution of the secondary peak at 101.6 eV is assigned to Si–N bonds.³⁶ The XPS core peaks (N 1s, Al 2p, C 1s, and O 1s) as well as the surface composition table for the sample after pretreatment and 20 cycle ALD are presented in Fig. S2 and Table S2 of the [supplementary material](#). These results, along with the EDX depth profiles of Fig. 5, show that indeed the Si substrate oxidation is reduced when introducing the $\text{N}_2\text{-NH}_3$ plasma pretreatment of the Si substrate prior to deposition.

DISCUSSION

Effect of the $\text{N}_2\text{-NH}_3$ plasma pretreatment on the initial deposition steps

Figure 3 shows that for the NPT Si substrates, a nucleation period exists before attaining the linear ALD regime. As previously said, this is due to the H-termination of the Si surface after the HF cleaning. The Si–H bonds are unreactive toward both ALD reactants.^{16,17} The deposition during the first ALD cycle initially takes place on surface defects,^{16,19} such as Si–OH or Si–O–Si groups, which were not removed during the HF cleaning of the substrate

and serve as nucleation sites. Although the HF pretreatment is able to remove the majority of SiO_x , certain surface defects remain on the surface but not in the form of a continuous layer. During the next cycle, the film is preferentially formed around and on the already deposited Al_2O_3 , leading to an island growth mode, up to the point where the islands coalesce and form a continuous film.^{18–20} Our results show that for the NPT substrates, the constant GPC of ~ 0.1 nm/cycle previously reported for the present ALD process¹³ is not yet achieved after 20 cycles, in consistent with the results of Puurunen *et al.*¹⁸ A detailed, experimental, and computational investigation of the initial deposition steps and the growth regime allowed concluding that an island growth regime takes place during the initial deposition steps.²⁰ From this analysis, it was shown that the initial concentration of surface defects was 0.08 groups/nm² and that 25 ALD cycles are needed in order to obtain a fully continuous film.

When performing the $\text{N}_2\text{-NH}_3$ plasma pretreatment, the deposition is enhanced during the initial ALD cycles. The results of Fig. 4 indicate that a constant GPC of ~ 0.1 nm/cycle is obtained even after 5 cycles. The film is continuous over the surface even after 5 cycles (Fig. 4).

Xu *et al.*²⁷ also reported a higher deposition during the first ALD cycles when using an NH_3 plasma pretreatment. However, in their study, the total thickness of the film observed by TEM is assumed to consist of Al_2O_3 , leading to a 6.7 nm film thickness after 35 ALD cycles. This value would imply a mean GPC of ~ 0.19 nm/cycle, which is almost two times the previously reported GPC of Al_2O_3 from TMA and H_2O .^{7,13,19} Once the Al_2O_3 film is continuous, the initial surface does not affect anymore the deposition and the process enters in its steady ALD regime. Hence, no surface pretreatment should affect the deposition once the system attains the linear ALD regime. In this work, we show [Fig. 1(a)] that the $\text{N}_2\text{-NH}_3$ plasma pretreatment results in an amorphous layer. The film thicknesses obtained in our present study reveal that after 5 cycles, the growth indeed reaches the ALD regime, with a constant GPC of 0.1 nm/cycle, in agreement with reported values from the literature^{7,19} as well as experimental and computational predictions performed for our ALD system in our previous work.¹³

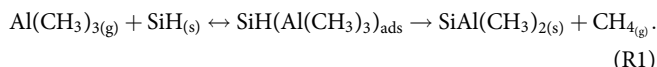
We now proceed to a literature review to explain the effect of the $\text{N}_2\text{-NH}_3$ plasma PT on the initial growth increase. Widjaja and Musgrave³² studied the nitridation of the Si surface under the exposure of NH_3 , using density functional theory (DFT) calculations. NH_3 adsorption is dissociative on the Si surface, leading to the formation of Si– NH_2 surface species.³² They showed that around 327 °C, further dissociation is possible, with the insertion of N in the Si–Si bonds.³² A combined experimental and theoretical study from Rodríguez-Reyes and Teplyakov³³ using DFT calculations and IR spectroscopy validate the above results, showing that the Si– NH_2 surface species start to dissociate between 227 and 327 °C to form $(\text{Si})_2\text{NH}$, in two different structures, bridged and backbonded,^{33,34} where neither of the two could be ruled out. In our case, as the exposure to $\text{N}_2\text{-NH}_3$ plasma is performed at 300 °C, we assume that all three structures could be formed: Si– NH_2 , which is not completely dissociated, and $(\text{Si})_2\text{NH}$ in both bridged and backbonded structures.^{33,34}

Lin and Teplyakov³⁵ studied the mechanisms occurring during TMA exposures of the Si surface using DFT calculations and computed energy barriers for TMA adsorption and reaction

on Si-H bonds. The authors performed the same study for TMA adsorption and reaction Si-NH₂ and (Si)₂NH bonds in both bridged and backbonded structures.³⁵ The considered mechanisms taken into account are the following:

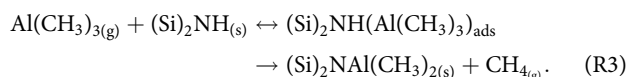
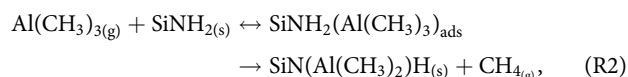
TMA on Si-H

Al(CH₃)₃ reversibly adsorbs on Si-H forming a weak Al-Si bond. The predominant reaction yields a surface Si-Al(CH₃)₂, with the desorption of CH₄. This reaction is considered irreversible. The mechanism is shown hereafter,



TMA on NH_x-terminated Si

Al(CH₃)₃ reversibly adsorbs on surface NH forming an Al-N bond. The reaction taking place yields a surface N-Al(CH₃)₂, with the desorption of CH₄. This reaction is considered irreversible. The above mechanism is shown below, for SiNH₂ and both of the two different (Si)₂NH structures,



Their results are presented in Fig. 7.

It shows that the deposition is favored for the three different NH bonds, compared to the Si-H bonds. TMA is found to adsorb more exothermically on the Si-NH_x bonds, than on the SiH ones. The overall energy barrier to reach the transition state is significantly smaller for the NH-terminated bonds, and the final products

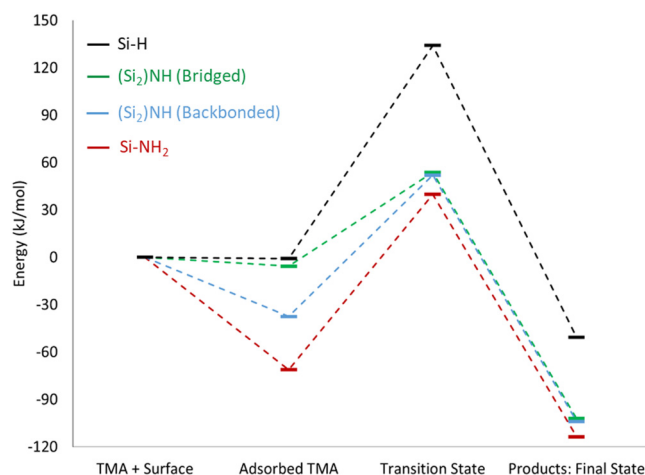


FIG. 7. Data from Lin and Teplyakov³⁵ for the deposition of TMA on Si with different surface terminations.

are in a much lower energy state. In particular, the NH₂ is the more favorable surface termination for the deposition of TMA, presenting the lower overall energy barrier, of 39.9 kJ/mol, while the reaction products are 113.7 kJ/mol lower in energy than the reactants.³⁵

We now perform a reaction probability study of an already adsorbed TMA molecule on the surface, in order to analyze the N₂-NH₃ plasma pretreatment effect on the TMA deposition kinetics. We calculate the reaction probability (p_{reaction}) of an adsorbed TMA molecule on the surface, by dividing its forward reaction rate (R_{reaction}) with the total rate of all possible events, which for the adsorbed TMA are forward reaction and desorption ($R_{\text{desorption}}$),

$$p_{\text{reaction}} = \frac{R_{\text{reaction}}}{R_{\text{reaction}} + R_{\text{desorption}}}. \quad (1)$$

Both mechanisms are assumed to follow first order Arrhenius kinetics. We assume the activation energy for desorption ($E_{\text{desorption}}$) to be equal to the energy released during the adsorption step. The forward reaction energy barrier (E_{reaction}) is the difference between the energies of the transition state and the adsorbed TMA state. By assuming that the preexponential factors for both reaction and desorption are equal, the reaction probability can be expressed as

$$p_{\text{reaction}} = \frac{e^{-\frac{E_{\text{reaction}}}{RT}}}{e^{-\frac{E_{\text{reaction}}}{RT}} + e^{-\frac{E_{\text{desorption}}}{RT}}}, \quad (2)$$

where R is the ideal gas constant and T the temperature.

The results for the reaction probabilities calculated at 300 °C are shown in Table I, using the activation energies computed by Lin and Teplyakov.³⁵

Results of Table I show a clearly higher reactivity of the Si-NH₂ and (Si)₂NH species toward the ALD reactants, in comparison with the Si-H species. An adsorbed TMA molecule has a reaction probability increased by more than seven orders of magnitude on NH-terminated surfaces than on the Si-H surface. Specifically, the highest reaction probability is computed on Si-NH₂.

It must also be noted that besides the TMA reactions with the PT surface, the H₂O reactions are also favored. The low reactivity of the H-terminated Si surface toward H₂O has been previously studied theoretically¹⁰ and experimentally.^{16,17} Brewer *et al.*²⁶ showed that on the NH₃ pretreated Si, deuterated water D₂O reacts and oxidizes the PT layer, even at temperatures as low as 190 °C. These reactions could lead to the formation of oxygen containing species, such

TABLE I. Reaction probabilities for the different surface bonds calculated at 300 °C, using the energies calculated by Lin and Teplyakov.³⁵

Surface termination	Reaction probability at 300 °C
Si-H	$6.0 \cdot 10^{-13}$
Si-NH ₂	$2.3 \cdot 10^{-4}$
(Si) ₂ NH (bridged)	$1.3 \cdot 10^{-5}$
(Si) ₂ NH (backbonded)	$1.8 \cdot 10^{-5}$

as Si–O–N or OH bonds on which TMA can chemisorb more favorably during the subsequent reactant exposure.

Effect of the $\text{N}_2\text{-NH}_3$ plasma pretreatment on substrate oxidation

Besides increasing the growth rate during the initial deposition cycles, the $\text{N}_2\text{-NH}_3$ plasma pretreatment is also effective in reducing the Si surface oxidation (Fig. 5). For the NPT Si surfaces, the interfacial oxide thickness remains close to 2 nm for all samples.

Such interfacial layer thicknesses have already been observed by Xu *et al.*²⁷ and Kaur *et al.*³⁰ We showed that for the NPT samples, the interfacial layer consists of Si oxides in multiple oxidation states, AlO_x species, and $\text{Si}_x\text{O}_y\text{Al}$.²⁰ It has been reported that it is formed by species interdiffusion and reaction through Al–OH defects in the film bulk.^{4,23} Si–OH bonds created during the island growth mode of the first cycles could also be a source of Si oxidation.²² The presence of such species has been evidenced for the NPT samples by SIMS analysis.²⁰ The Si oxidation during the nonfull coverage of the surface by Al_2O_3 islands has also been reported by Xu *et al.*²⁴ and has been overcome by applying long TMA exposures of the Si substrate prior to deposition.

In the case of the PT Si surfaces, our results indicate that for all samples, the substrate oxidation is significantly reduced. This shows that the PT layer along with the ALD deposited film serve as an effective barrier toward the oxidation of the Si substrate. This substrate oxidation reduction has been previously reported by Brewer *et al.*,²⁶ as well as by Xu *et al.*,²⁷ who reported low interface oxidation. In their work, Brewer *et al.*²⁶ exposed the NH_3 pretreated Si surfaces to D_2O . They reported that although D_2O oxidizes the formed Si_xN_y layer even at modest temperatures, the substrate surface beneath it is not oxidized. This shows that the pretreatment formed layer protects the Si surface from oxidation. Results of Figs. 1(b), 5, and 6 validate these observations. To determine whether the oxidized Si_xN_y interface of the PT samples presents better interfacial properties than the SiO_x and $\text{Si}_x\text{O}_y\text{Al}$ interface of the NPT samples, electrical characterizations should be performed, which are off the scope of the present study. Xu *et al.*²⁷ have shown that Al_2O_3 films grown on $\text{N}_2\text{-NH}_3$ plasma pretreated Si present better thermal stability, lower leakage current, and smaller CV hysteresis.

CONCLUSION

In this work, the effect of an *in situ* plasma $\text{N}_2\text{-NH}_3$ pretreatment of the Si (100) substrate prior to Al_2O_3 ALD from TMA and H_2O is thoroughly investigated both experimentally and theoretically, considering literature results. This pretreatment leads to significant deposition increase during the first ALD cycles, as observed by STEM images and EDX measurements. This is explained by the fact that the pretreated surface consists of Si– NH_2 and $(\text{Si})_2\text{NH}$ groups, which are considerably more reactive toward TMA than the H-terminated Si surface formed during the standard HF cleaning of the Si substrate. The substrate inhibition leading to island growth is then reduced, and a constant GPC is reached after 5 ALD cycles, instead of tens of cycles without such pretreatment. This pretreatment is also effective in reducing substrate oxidation. The interfacial oxide layer is ~ 2 nm for the nonpretreated samples,

while no SiO_x layer is detected for the samples with pretreatment. The amorphous layer formed by the pretreatment serves as an effective protective layer for the Si surface, as was shown by EDX and XPS characterizations. Although this layer is itself oxidized, the Si surface oxidation is reduced, which should improve the dielectric behavior, according to results reported for similar Si_xN_y interfaces.

This study shows that two of the main disadvantages of Al_2O_3 ALD from TMA and H_2O on Si, i.e., initial deposition inhibition and the growth of the interfacial SiO_x layer, can be reduced by using an appropriate Si surface pretreatment. This approach can be applied to other ALD materials, such as the promising high-k HfO_2 , presenting the same drawbacks. The achievement of deposition of continuous nanometric dielectric films with abrupt interfaces with Si could allow ALD to answer to the increasing demand of nanoelectronic device integration.

SUPPLEMENTARY MATERIAL

See the [supplementary material](#) for a detailed discussion of the N 1s, C 1s, and O 1s XPS core level peak and the surface composition obtained for the pretreated samples without ALD and with 20 cycle ALD.

ACKNOWLEDGMENTS

This work was partly funded by a Toulouse Tech Inter Lab 2016 grant and a Toulouse INP support. G.P.G. acknowledges the financial support by the NTUA Research Committee. We are indebted to C. Josse, A. Pugliara, and T. Hungria (UMS Castaing) for their help with sample characterizations and to H. Martinez (IPREM, Pau) for allowing timely XPS characterizations and for advice in the interpretation of the XPS spectra.

REFERENCES

- 1R. W. Johnson, A. Hultqvist, and S. F. Bent, *Mater. Today* **17**, 236 (2014).
- 2S. M. George, *Chem. Rev.* **110**, 111 (2010).
- 3R. L. Puurunen, *J. Appl. Phys.* **97**, 121301 (2005).
- 4O. Renault, L. G. Gosset, D. Rouchon, and A. Ermoloeff, *J. Vac. Sci. Technol. A* **20**, 1867 (2002).
- 5R. W. Wind, F. H. Fabreguette, Z. A. Sechrist, and S. M. George, *J. Appl. Phys.* **105**, 074309 (2009).
- 6V. Vandalon and W. M. M. Kessels, *Appl. Phys. Lett.* **108**, 011607 (2016).
- 7V. Vandalon and W. M. M. Kessels, *J. Vac. Sci. Technol. A* **35**, 05C313 (2017).
- 8R. C. Longo, J. H. G. Owen, S. McDonnell, D. Dick, J. B. Ballard, J. N. Randall, R. M. Wallace, Y. J. Chabal, and K. Cho, *J. Phys. Chem. C* **120**, 2628 (2016).
- 9Y. Widjaja and C. B. Musgrave, *Appl. Phys. Lett.* **80**, 3304 (2002).
- 10M. D. Halls and K. Raghavachari, *J. Chem. Phys.* **118**, 10221 (2003).
- 11A. S. Sandupatla, K. Alexopoulos, M.-F. Reyniers, and G. B. Marin, *J. Phys. Chem. C* **119**, 13050 (2015).
- 12C. D. Travis and R. A. Adomaitis, *Chem. Vap. Deposition* **19**, 4 (2013).
- 13G. P. Gakis, H. Vergnes, E. Scheid, C. Vahlas, A. G. Boudouvis, and B. Caussat, *Chem. Eng. Sci.* **195**, 399 (2019).
- 14G. P. Gakis, H. Vergnes, E. Scheid, C. Vahlas, B. Caussat, and A. G. Boudouvis, *Chem. Eng. Res. Des.* **132**, 795 (2018).
- 15P. Peltonen, V. Vuorinen, G. Marin, A. J. Karttunen, and M. Karppinen, *J. Vac. Sci. Technol. A* **36**, 021516 (2018).
- 16M. M. Frank, Y. J. Chabal, M. L. Green, A. Delabie, B. Brijs, G. D. Wilk, M.-Y. Ho, E. B. O. Da Rosa, I. J. R. Baumvol, and F. C. Steidle, *Appl. Phys. Lett.* **83**, 740 (2003).

- ¹⁷M. M. Frank, Y. J. Chabal, and G. D. Wilk, "Nucleation and interface formation mechanisms in atomic layer deposition of gate oxides," *Appl. Phys. Lett.* **82**, 4758 (2003).
- ¹⁸R. L. Puurunen, W. Vandervorst, W. F. A. Besling, O. Richard, H. Bender, T. Conard, C. Zhao, A. Delabie, M. Caymax, S. De Gendt, M. Heyns, M. M. Viitanen, M. De Ridder, H. H. Brongersma, Y. Tamminga, T. Dao, T. De Win, M. Verheijen, M. Kaiser, and M. Tuominen, *J. Appl. Phys.* **96**, 4878 (2004).
- ¹⁹R. L. Puurunen and W. Vandervorst, *J. Appl. Phys.* **96**, 7686 (2004).
- ²⁰G. P. Gakis, C. Vahlas, H. Vergnes, S. Dourdain, Y. Tison, H. Martinez, J. Bour, D. Ruch, A. G. Boudouvis, B. Caussat, and E. Scheid, *Appl. Surf. Sci.* **492**, 245 (2019).
- ²¹M. D. Groner, J. W. Elam, F. H. Fabreguette, and S. M. George, *Thin Solid Films* **413**, 186 (2002).
- ²²V. Naumann, M. Otto, R. B. Wehrspohn, and C. Hagendorf, *J. Vac. Sci. Technol. A* **30**, 04D106 (2012).
- ²³L. G. Gosset, J.-F. Damlencourt, O. Renault, D. Rouchon, P. Holliger, A. Ermoloeff, I. Trimaille, J.-J. Ganem, F. Martin, and M.-N. Séméria, *J. Non. Cryst. Solids* **303**, 17 (2002).
- ²⁴M. Xu, C. Zhang, S.-J. Ding, H.-L. Lu, W. Chen, Q.-Q. Sun, D. W. Zhang, and L.-K. Wang, *J. Appl. Phys.* **100**, 106101 (2006).
- ²⁵J.-F. Damlencourt, O. Renault, A. Chabli, F. Martin, M.-N. Séméria, and F. Bedu, *J. Mater. Sci. Mater. Electron.* **14**, 379 (2003).
- ²⁶R. T. Brewer, M.-T. Ho, K. Z. Zhang, L. V. Goncharova, D. G. Starodub, T. Gustafsson, Y. J. Chabal, and N. Moumen, *Appl. Phys. Lett.* **85**, 3830 (2004).
- ²⁷M. Xu, C.-H. Xu, S.-J. Ding, H.-L. Lu, D. W. Zhang, and L.-K. Wang, *J. Appl. Phys.* **99**, 074109 (2006).
- ²⁸H.-L. Lu, M. Xu, S.-J. Ding, W. Chen, D. W. Zhang, and L.-K. Wang, *J. Mater. Res.* **22**, 1214 (2007).
- ²⁹H. Takeuchi and T.-J. King, *Appl. Phys. Lett.* **83**, 788 (2003).
- ³⁰G. Kaur, N. Dwivedi, X. Zheng, B. Liao, L. Z. Peng, A. Danner, R. Stangl, and C. S. Bhatia, *IEEE J. Photovolt.* **7**, 1224 (2017).
- ³¹S. W. Lim, F. Machuca, H. Liao, R. P. Chiarello, and R. C. Helms, *J. Electrochem. Soc.* **147**, 1136 (2000).
- ³²Y. Widjaja and C. B. Musgrave, *Phys. Rev. B Condens. Matter Mater. Phys.* **64**, 205303 (2000).
- ³³J. C. F. Rodríguez-Reyes and A. V. Teplyakov, *Phys. Rev. B Condens. Matter Mater. Phys.* **76**, 075348 (2007).
- ³⁴J. C. F. Rodríguez-Reyes and A. V. Teplyakov, *J. Phys. Chem. C* **111**, 16498 (2007).
- ³⁵J.-M. Lin and A. V. Teplyakov, *Theor. Chem. Acc.* **132**, 1404 (2013).
- ³⁶A. R. Chourasia and D. R. Chopra, *Surf. Sci. Spectra* **2**, 117 (1993).